Laser warning and pointed optics detection using an event camera

Nicolas Boehrer, Hugo J. Kuijf, Judith Dijk TNO, PO Box 96864, 2509JG The Hague, The Netherlands

Abstract. The detection of a threat before launch offers the best options to avoid the threat. However, detecting a threat before it concretizes remains a difficult task because of the obvious risk of error. The detection of a laser emission or of optics that are pointed towards the platform gives a significant cue of a hostile behaviour. In our work, we investigate if and how event (also called neuromorphic) cameras can be used to detect laser emission and combined with a laser source to detect retro-reflections caused by pointed optics. We explore how the high temporal resolution of the event stream can be used to extract temporal information on the laser signal. The approach is demonstrated for a laser warning receiver use-case and a retro-reflection detection configuration using data that was collected during the DeBeLa trial in Germany and that reproduce operationally relevant scenarios.

Keywords: event camera, neuromorphic imaging, retro-reflection, laser warning

1 INTRODUCTION

Threat detection

Recent military platforms are equipped with active protection systems designed to defeat incoming threats by disturbing its guidance (soft kill) or by physically interacting with it (hard kill). However, due to the novel missile developments, it has become increasingly difficult to build systems combining a fast reaction time and an accurate prediction of the threat trajectory. We investigate here an alternative approach consisting of detecting the threat before the actual launch. By detecting a threat before it's launch, one maximizes the amount of options available to react to the threat and the performance of the chosen counter measure. In this paper, we focus on methods relying on electro-optical (EO) sensors for the detection of hostile elements in the vicinity of the platform. Over the years, different detection methods have been proposed. All methods rely on the detection of a form of signature specific to the hostile element, such as the 3D shape of the launcher [1], the polarization of the light reflected by artificial surfaces [2] [3] [4] [5], the laser emission generated by the launcher, the retro-reflection (also known as cat-eye effect) produced by an optical setup pointed in the direction of the platform [6] [7] when illuminated with a laser.

In this article, we are focusing on two use cases, first, the detection of the laser emitted by the launcher before firing such as a laser warning receiver and, then, the detection of pointed optics using the principle of retro-reflections.

Before launch, lasers might be used for two purposes. They are used to measure the range between the launcher and the target (laser rangefinder) and they are used to illuminate and designate the target. The goal of the laser emission detection is to detect the presence of a laser, determine the location of the source, and potentially identify the type of threat based on a laser signature. Laser sources capable of performing at long distance may differ in wavelength and pulse patterns. Aside from the accurate localization and identification of the threat, laser warning receivers should also provide a 360° coverage around the platform, a detection range superior to 5 km, a fast response time and a low false alarm rate combined with a reduced size, weight and power (SWaP) footprint. Laser warning receivers are produced by different industry actors such as, for instance, Hensoldt [6], Thales [7] or Elbit Systems [8].

Pointed optics can potentially be detected by illuminating the zone where the optics is present using a laser flood illumination. A small part of the laser illumination is reflected by the optical components and by the focal plane of the observing device. The retro-reflection detection can be used to detect observation devices (scopes, binoculars), imagers, and seekers. Some strategies were devised by [9] [10] to reduce the laser cross section of EO systems. Aside from the detection and localization, retro-reflections also offer possibilities to retrieve additional information about the source and about the threat. The analysis of the response across different spectral bands allows to derive features that are specific to threats. With a detector providing enough temporal resolution and sensitivity, one can also measure the full waveform of

the laser signal returned by each optical interface in front of an imager or measure temporal patterns. Those retro-reflection features can be used to distinguish between rotating reticle-based seekers and imaging-based seekers.

Both applications require a detector that offers enough sensitivity to capture potentially weak signals without suffering from the background illumination. Because of the pulsed nature of most laser signals and given the short pulses (usually a few ns), detectors need to provide a high temporal resolution. Currently, different types of sensors exist. Scientific CMOS (sCMOS) offers a wide range of sensor options in Si (VIS-NIR) and InGaS (SWIR) with small pixel pitch (4 μ m). With that technology, the sensor integrates photons during a fixed time interval that can be synchronized with an active illumination trigger signal. In the case of a laser warning receiver, the laser signal is emitted by the opponent and the pulses cannot be controlled. The SWaP and data generation rate of high-speed camera systems usually prevents from using them to measure temporal features of the laser signal.

In this paper we will study the use of an event camera (also known as neuromorphic camera) [11] to detect and record laser signals. This new type of camera does not record an entire frame with a global shutter clock but instead outputs an asynchronous stream of intensity changes, so-called events. Contrary to classical frame recordings that record a lot of redundant data for image regions that stay constant over time, this new recording technique allows for recording of only the local changes between frames, so the bandwidth and the recording resources are best used to record the local dynamics of the scene or of the camera. When combined with a computer vision algorithm like optical flow [12] [13] [14], visual odometry [15] [16], 3D reconstruction [17], this new paradigm shows advantages for dynamic scenes, see [18] for an extensive overview.

With its low latency, log sensitivity, and high temporal sampling, the event camera is expected to be well suited to record the temporal variations of a pulsed laser source. The concept of event camera is summarized in Section 2. Section 3 presents the methods and setups used for the experiments. In this paper we will study two possible operational use cases. First, the laser warning configuration (labeled LW in the rest of the paper). In this configuration the camera is placed on the target side and is directly illuminated by the laser. Then, the retro-reflection use case (which is labeled RR), with the camera placed next to the laser to detect retro-reflection on pointed optics. Section 4 presents the results and finally, the conclusions are summarized in Section 5.

2 EVENT BASED IMAGING

Unlike conventional cameras that record entire frames synchronously, event cameras only record logarithmic intensity changes. The event camera encodes the changes as an asynchronous series of spikes called events.

$$e_k = (u_k, t_k, p_k)$$

where the k-th event e_k is a quadruplet that consists of an image location $\mathbf{u}_k = (x_k, y_k)^T$, a polarity p_k (positive or negative direction), and a time stamp t_k . The pixel operation of an event camera is shown in Figure 1. An event is produced when the difference between the memorized log intensity (on top, the thin blue line) and the current log intensity (on top, the thick blue line) exceeds a certain threshold C (controlled by the user). When the threshold is passed, the time stamp, the pixel position, and the polarity is emitted, and the current log intensity value is memorized for the monitoring.

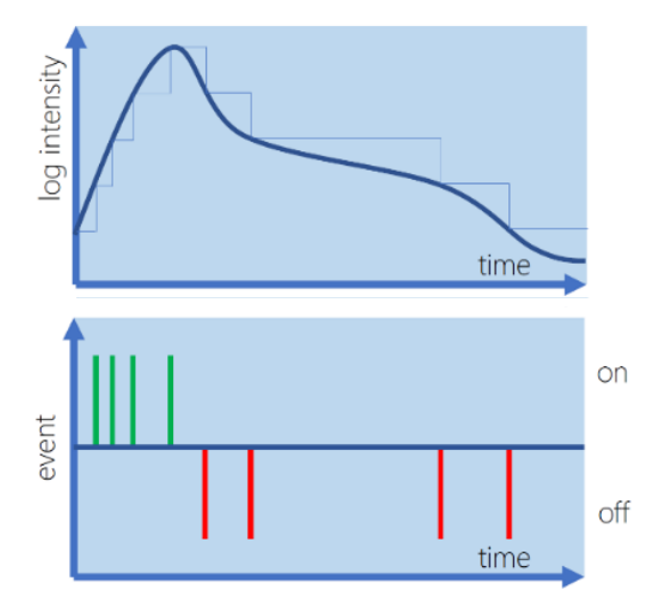


Figure 1: Pixel operation of an event camera. On top, the log intensity received by a pixel over time. At the bottom, the resulting events emitted by the pixel.

The asynchronous event stream can be converted into a classical frame by integrating events over a time interval. This method is mostly used to visualize the event stream and assess the signal level available for a detection algorithm. The event count map N is generated by counting for each pixel i and out of a total of m events, the number of events that occurred at the location of pixel i, such that each pixel n_i in the event count map encodes:

$$n_i = \sum_{k=0}^m \delta(u_i - u_k)$$

In order to extract spectral features from an event stream, one must compute the corresponding frequency spectrum. To compute the frequency spectrum, we follow the method proposed by [19] which is shown in Figure 2. One first creates a signal by defining a temporal bin size. Based on each event time stamp t_k one associates the proper bin and integrates the event polarities p_k to create an event vector. One can then derive the frequency spectrum by computing the fast Fourier transform (FFT) of the event vector.

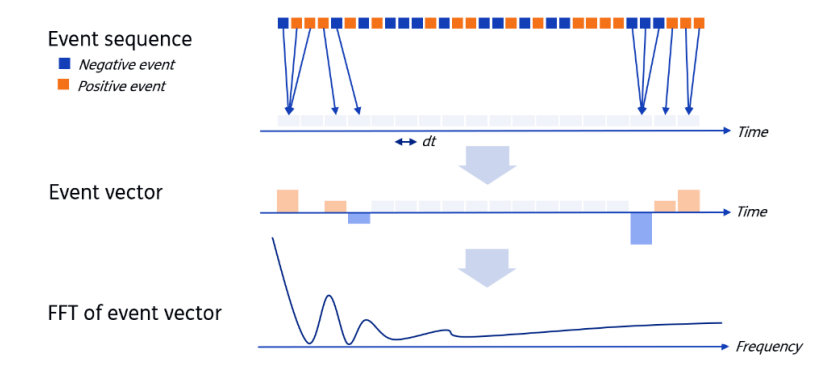


Figure 2: The computation of the fast Fourier transforms of the event sequence

3 METHODS

Data collection

To validate the detection of a laser source and of retro-reflection with an event camera, a dataset was collected during the trial performed for the European Defence Agency project Detect Before Launch (DEBELA) (PRJ-RT-829). The trial took place in June 2023 in Oberjettenberg in Germany and was organized by the Wehrtechnische Dienststelle für Schutz- und Sondertechnik (WTD 52). The test range spreads from the top of a mountain, where a measurement hut is placed to a valley in which target objects or camera systems are placed. Figure 3 shows a schematic overview of the trial range and illustrates the two configurations that were used for both experiments.

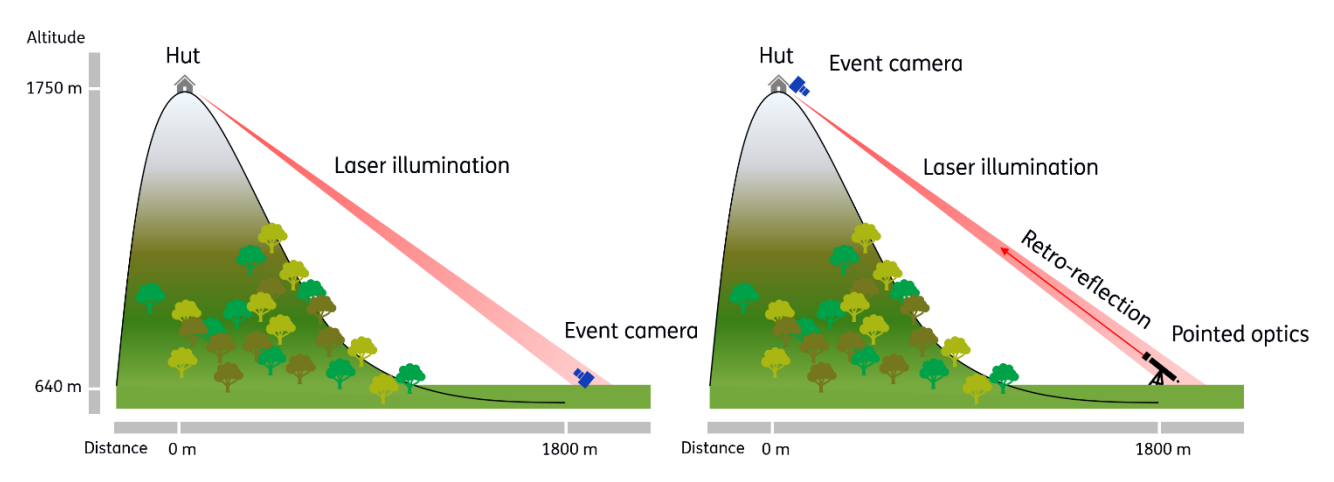


Figure 3: Left, schematic view of the data collection principle for the laser warning receiver (LW) and right for the retro-reflection (RR)

In the laser warning receiver configuration LW (left), the laser is placed in the hut and illuminates the target area in the valley where the event camera is placed. In the retro-reflection configuration RR (right), the laser source in the hut illuminates target objects in the valley, and the event camera, next to the laser, records the retro-reflection.

Setup

The setup is shown in Figure 4 and consists of a NIR laser source and an event camera attached to a telescope. In order to perform measurements at long distance, the laser energy is concentrated on a narrow vertical strip that is scanned horizontally to illuminate the entire field of view. This scanning slit can be synchronized with a classical frame-based camera to perform optics detection. With the setup presented here, we leverage the asynchronous temporal sampling of the event camera that does not require a synchronization with the scanning cycles.



Figure 4: Picture of the setup, used here for the retro-reflection experiment. For the clarity of the picture, the event camera was moved to the left while taking the picture. During measurements, it was as close to the laser as possible.

The event camera (IniVation DAVIS346) has an array size of 346x260 pixels and a pixel pitch of 18.5 μm . In the LW setup, the camera was equipped with a zoom lens offering a wide field of view and a variable diaphragm (Sigma 70-200 f/2.8). In the RR configuration, the laser and camera were kept at a short distance of 20 cm. The camera was equipped with a compact Schmidt-Cassegrain telescope (Celestron C5) with a focal length of 1250 mm and an aperture of f/10. The main specifications of the hardware used in the setup are summarized in Table 1.

Table 1: Main hardware specifications used in the setup

Laser source (LW & RR)	
Wavelength	0.8 μm
Pulse energy	0.2 mJ
Average power	200 mW
Repetition rate	1 kHz
Beam divergence	0.8 x 38 mrad
Scanning rate	25 Hz
Camera (LW & RR)	
Array size	346 x 260 pixels
Pixel pitch	18.5 μm
Central wavelength	550 nm
Quantum efficiency	25% @ 550 nm / 15% @ 800 nm
Dimensions L x H x D	60 x 40 x 24.5 mm
Weight	100 g
Power consumption	10 - 30 mW
Optics (LW)	
Focal length	25 mm (wide) / 200 mm (narrow)
Aperture diameter	17 mm (wide) / 71 mm (narrow)
IFOV	264,2 μrad – 92.5 μrad
Optics (RR)	
Focal length	1250 mm
Aperture diameter	125 mm
IFOV	14,8 µrad

4 EXPERIMENTS & RESULTS

This section presents the results of our experiments that intend to evaluate the suitability of the event camera for the detection of laser sources and retro-reflections in real conditions. First, for the laser warning configuration (LW), we verify

that the event camera is sensitive enough to detect the NIR laser emission over a range of 2km. We study the influence of the illumination onto the visibility of the laser source. Then, we evaluate the effect of camera vibrations onto the visibility of the laser source. Finally, the setup is placed in a RR configuration and we evaluate the visibility of the laser retroreflection after a pulse roundtrip of 4km.

Laser warning (LW)

The camera responds to log-intensity changes and therefore we expect the camera to react to smaller intensity changes in dark conditions than for a bright background illumination. To verify this behaviour, we placed the event camera in the valley and recorded the laser while illuminating the camera. We measured the event camera response to the direct illumination using a narrow field of view lens and varied the intensity by changing the lens aperture. The lens was chosen to have a vignetting and sharpness variations over the aperture range below 2% in the center of the field of view [20]. The data collection was performed rapidly (1 min) such that outdoor illumination remains identical between the sequences.

Figure 5 compares the heatmaps (overlaid with an intensity frame) of the event rate and recorded while reducing the lens aperture size. The smallest aperture (f/16.0) was chosen such that the blur induced by diffraction and the corresponding Airy disk size remains under 1 pixelOne can observe that the amount of light reaching the sensor is reduced (the background image gets darker with the f#). In the figure, one can notice that the spot size corresponding to the laser source in the hut increases considerably when comparing the widest and the smallest aperture. This behaviour is especially noticeable between f/5.6 and f/8.0.



Figure 5: The event rate heatmap for different aperture sizes. From left to right, f/2.8, f/4.0, f/5.6, f/8.0, f/11.0 and f/16.0.

This behaviour can be quantified by comparing the event rate (in events/s) for the image area around the spot center. The result is shown in Figure 6, which shows a cross section of the spot and compares the event rate corresponding to the different apertures.

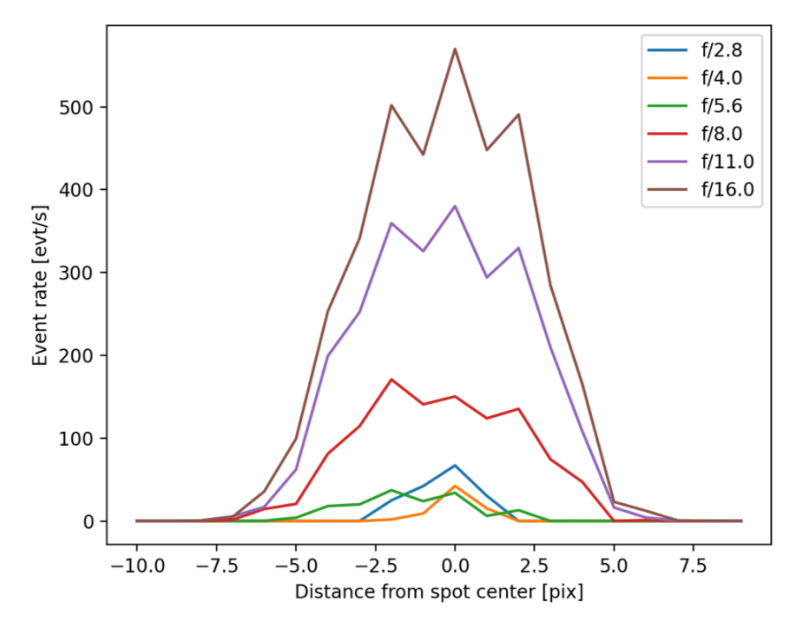


Figure 6: The event rate measured around the laser spot for different aperture sizes.

The figure shows that all spots are centered around the same point and that their respective width varies with the f#. For the smallest apertures, side lobes around the center of the spot are visible. With the IFOV (Table 1) and the spot width (10 pix) one could derive a measured beam divergence of 0.92 mrad, close to the 0.8 mrad of the laser specifications. The remaining error may be explained by slight inaccuracies in the focusing of the lens.

We compared the frequency spectrums of the laser signals recorded with the smallest and the largest apertures (f/16.0 and f/2.8 respectively). The result is shown in Figure 7.

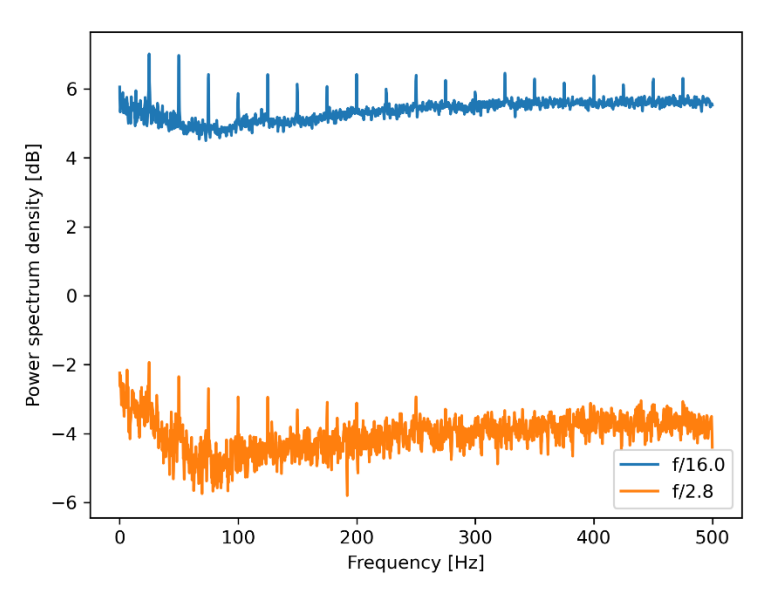


Figure 7: Comparison of the frequency spectrums of the recordings made with the largest and smallest lens apertures

The figure confirms the overall signal strength being stronger (+5.5dB) for a low sensor illumination than for the large aperture (-4dB) and the stronger illumination. The frequency analysis also shows that the laser signal a base frequency of

25Hz with higher harmonics. The sharp peaks corresponding to this frequency comb can be best distinguished in the recording made with the f/16.0 aperture. However, one can also observe that the same signal is also present in the recording made with the f/2.8 aperture. For the latter, the higher harmonics above 250 Hz cannot be distinguished from the noise. The base frequency of 25Hz corresponds to the scanning frequency of the mirror and the higher harmonics correspond to discontinuities in the time signal such as for square wave or triangle wave signals.

With this result, we can conclude that the event camera is sensitive enough to detect a pulsed NIR laser at 2km distance. The visibility of the laser source is improved by the reducing the lens aperture, allowing to measure a beam profile and estimate a beam divergence that is close to the expected one. The spectral analysis allows to retrieve the frequency and the wave pattern used for the scanning.

Laser warning (LW) with camera vibrations

In an operational context, the camera is expected to move. The camera motion will produce a displacement of the edges of scene in the image. The edge displacements will cause intensity variations and the event camera trigger events that are not related to the laser source. One could argue that shocks and vibrations will generate high frequent events around the edges of the scene, which may disturb the detection of the laser pulses.

To evaluate the influence of vibrations, we equipped the camera with a lens with a wide field of view and placed it in the valley at the same location as the one used in the previous experiment. In some of the sequences, vibrations were introduced by hitting the tripod while recording the NIR laser source in the hut.

Figure 8 shows in the top row, on the left, the background intensity image recorded by the camera. The mountain with the measurement hut is in the center of the field of view but no NIR source can be identified in this image. In the center, the heatmap overlaid with the background image, displays the event rate. A clear spot is visible at the top of the hill. The spot corresponds to the laser location. On the right, the figure shows the detection mask corresponding to the detected spot.

In the bottom row of the figure, one can observe the same pictures as for the top row but for a sequence recorded with vibrations. On the left, one can notice that the laser spot is still not visible in the background intensity image. In the center, it is visible that events are generated around the edges of the mountain, which have enough contrast to generate events. However, when comparing the edges and the laser activities shown by the heatmap, one can observe that the laser spot generates events at a much larger rate than the mechanical vibrations that may affect the camera. The right part of the image, shows that the laser spot detection is unaffected by the vibrations and still marks the same location as for the sequence without vibrations.

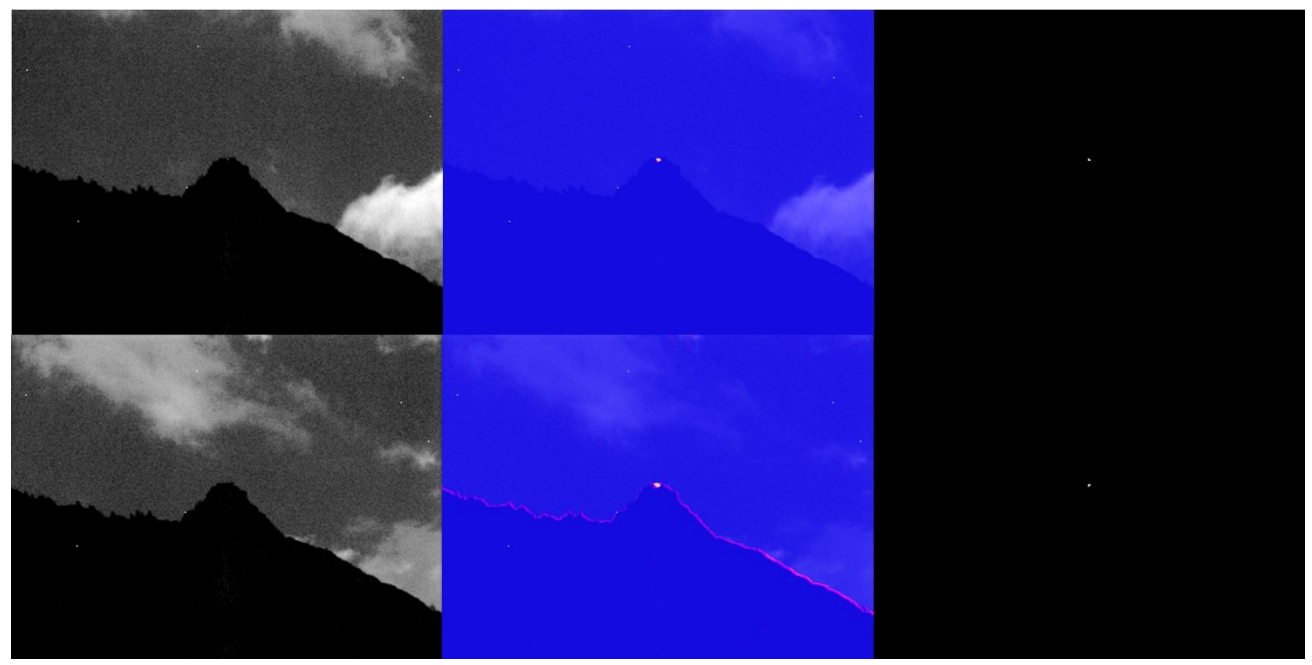


Figure 8: Events response to a direct laser illumination recorded with a wide field of view (f=25mm). From left to right, the intensity image, the number of events, the laser spot detection. Without camera motion (top row) and with camera motion (bottom row).

Another method to distinguish the events produced by the laser source from the events produced by the camera motion is to extract the temporal patterns present in the event trains.

We compared the power spectrum density (PSD) of a part of the image where the laser source is present and produces events to a zone where the events are generated by the camera motion and the contrasted edge. The result is shown in Figure 9. When looking at the event frequency spectrum corresponding to an edge (orange curve), one can see a flat PSD when no motion is present since no events are generated. When motion is present, the energy is mostly located in the area under 50 Hz. Above 150 Hz, the PSD is flat and no specific frequency peaks out. When looking at the PSD of the events generated by the laser source, one can observe the same pattern with the 25Hz base frequency as shown in the previous experiment. This specific pattern, produced by the scanning mechanism, is also visible on the spectrum corresponding to the footage recorded with motion. In the latter, the average amount of energy increases since it contains more events due to the vibrations. Since the laser location in the image is also affected by motion, the global shape of the spectrum corresponding to the laser (blue) follows the one corresponding to the event stream produced by the edge (orange) with most of the shake energy located under 50Hz. However the 25Hz frequency comb is not visible on the spectrum corresponding to the edge and remains specific to the laser.

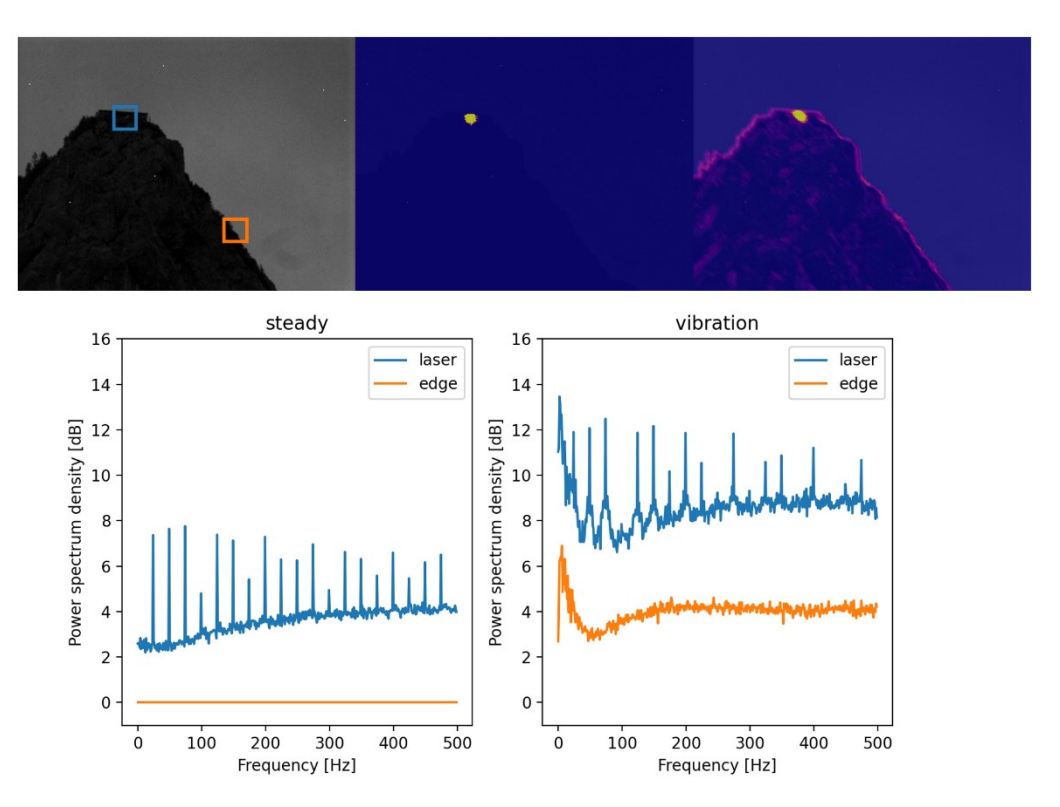


Figure 9: Comparing the frequency spectrums of events generated by the laser to the events generated by motion.

Top row from left to right, the background and the crop locations, the event count image when no motion is present, the event count image when camera motion is present. Bottom row, from left to right, the PSD corresponding to the crops of the footage without motion and the PSD of the crops of the footage with motion.

This experiment outlines two possible approaches to reliably detect the laser source and to distinguish it from the events generated by the own camera motion. The first method, intensity based, relies on the assumption that a pulsed laser will generate a larger amount of events than the own camera motion due to the high repetition rate of the laser (1kHz in this experiment). This event activity cannot be reached by normal camera motion. The second method outlines the presence of spectral features such as the scanning mechanism in this experiment. Those spectral features are specific to the laser source and can be detected by applying banks of filter combs designed to detect the modulation induced by a scanning mechanism (or a different mechanism such as a rotating reticle).

Retro-reflection (RR)

We evaluated the possibility to detect retro reflections using an event camera. As described in the previous section, the NIR laser was used to shine from the measurement hut onto a 1" corner cube that simulates an ideal optics pointed onto the measurement hut. The laser light reflected by the cube in the direction of the laser source was recorded using an event camera, placed in the measurement hut. Figure 10 shows the result of the retro-reflection detection over a range of 2 km.



Figure 10: The laser retro-reflection captured by an event camera, from left to right, the background, the event rate heatmap overlapped with the background image, and the detection mask

In the figure, one can see that the laser retro-reflection is clearly visible in the center of the corner cube reflector. Similarly to the previous section, this confirms the visibility of the laser signal after a round trip distance of 4000 m. For real optical setups pointed towards the camera, the visibly of the spot will depend on the optics aperture and its focus. With our setup, the reflector is passive, and no element is expected to change the temporal pattern of the laser signal.

To validate this, we extracted the PSD of the event stream generated by the retro-reflection. The result is shown in Figure 11. One can observe the same pattern as for the direct illumination, with a sequence of peaks, equally spaced by 25 Hz, corresponding to the scanning rate of the laser.

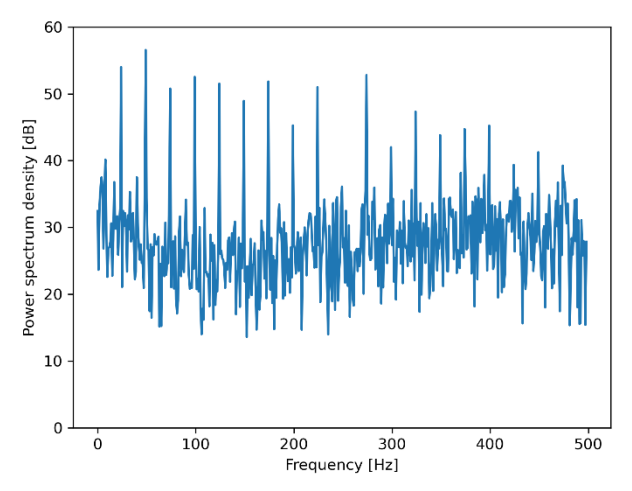


Figure 11: The power spectrum density of an event stream produced by the laser retro-reflection on a corner cube reflector placed at 2000 m.

This experiment shows that the event camera can record a retro-reflected signal that carries the same spectral characteristics as the ones observed for the direct illumination. This spectral pattern can here as well be used to enhance the robustness of the retro-reflection detection.

5 CONCLUSION

In this paper, we presented a new approach for early threat detection. The new concept relies on using an event camera to detect a laser emission or to record retro-reflections. We have shown that this new type of camera can detect a laser source at distance (2 km). In our experiment, the detection sensitivity increased when the illumination was reduced, leveraging the log sensitivity of the device. We have also shown that the temporal resolution of the sensor allows to record the temporal patterns associated with the laser emission. This information can be used to distinguish the laser source from other sources of events such as the own camera motion or vibration. Furthermore, the ability to record a temporal signature of the laser

after, for instance a retro-reflection, also allows to improve the robustness of the detection and potentially classify the type of threat (for instance for rotating wheel seekers).

This capability of recording temporal signatures with imager systems is quite novel and was up to now only possible using high speed cameras. The practical use of high-speed camera is limited by their SWaP (size, weight, and power) footprint, the strong illumination requirement, and the generation of an important quantity of redundant data that must be processed in order to detect threat. The novelty of the approach presented in this paper resides in the asynchronous sensing paradigm. The event camera provides a solution that natively adapts to the scene dynamics, allowing to combine the temporal sensing capability with a low SWaP (volume of 0.058L, weight of 100g, a maximum power consumption of 30 mW, see Table 1 for more details) and a sparse data generation.

One of the main limitations for an actual use for threat detection is the chip availability for infra-red wavelengths. Currently, event cameras chips are only available in the sensitivity range of the silicon (for wavelengths between 300 and 1100 nm), up to the near infrared. There is no fundamental limit to use the event read-out technology in other spectral bands of interest. With hybrid bonding, manufacturers are capable of combining different materials for the detector part and the read-out part of a same chip. InGaS-based sensors for short wave infrared (SWIR) and later, variants for thermal infrared are expected to appear on the market and address the gap.

Nevertheless, this first study shows the strong potential of event cameras for laser warning receiver and retro-reflection detection. We have shown that the high temporal resolution, the low data bandwidth and the small SWaP offered by this technology could allow to build robust low latency early detection systems. Moreover the reduced SWaP allows this technology to be used not only for large platforms but also on light-weight platforms such as quadcopters or wearables and enabling new disruptive applications.

6 REFERENCES

- [1] Q. Zheng, S. Der and R. Chellappa, "Model-based target recognition in pulsed ladar imagery," in *Proceedings. 1998 IEEE Computer Society Conference on Computer Vision and Pattern Recognition (Cat. No.98CB36231)*, 1998, pp. 515-520.
- [2] L. Le Hors, P. Hartemann and S. Breugnot, "Multispectral polarization active imager in the visible band," in *Laser Radar Technology and Applications V*, SPIE, 2000, pp. 380-389.
- [3] D. A. Lavigne, M. Breton, G. Fournier, J. F. Charette, M. Pichette, V. Rivet and A.-P. Bernier, "Target discrimination of man-made objects using passive polarimetric signatures acquired in the visible and infrared spectral bands," in *Polarization Science and Remote Sensing V*, SPIE, 2011, p. 816007.
- [4] N. Vannier, F. Goudail, C. Plassart, M. Boffety, P. Feneyrou, L. Leviandier, F. Galland and N. Bertaux, "Active polarimetric imager with near infrared laser illumination for adaptive contrast optimization," *Applied optics*, vol. 54, no. 25, pp. 7622-31, 2015.
- [5] A. L. Mieremet, R. (. Schleijpen and P. Pouchelle, "Modeling the detection of optical sights using retro-reflection," in *Laser Radar Technology and Applications XIII*, 2008.
- [6] Hensholdt, "ALTAS Advanced Laser Threat Alerting System," Hensholdt, [Online]. Available: https://www.hensoldt.net/products/optronics/altas-advanced-laser-threat-alerting-system/. [Accessed 01 2024].
- [7] Thales, "Land Survivability Laser Warning Detector: LWD," Thales, [Online]. Available: https://www.thalesgroup.com/en/worldwide/defence/land-survivability-laser-warning-detector-lwd. [Accessed 01 2024].

- [8] E. Systems, "Laser Warning Systems," Elbit Systems, [Online]. Available: https://elbitsystems.com/product/laser-warning-systems-lws/. [Accessed 01 2024].
- [9] Q. Ye, Y. Wu, Y. Li, H. Zhang, L. Wang and X. Sun, "A Retroreflection Reduction Technique Based on the Wavefront Coded Imaging System," *Crystals*, vol. 11, no. 11, 2021.
- [10] A. Mieremet, R. Schleijpen, F. van Putten and H. Veerman, "Retroreflection reduction by masking apertures," *Optical Engineering*, vol. 49, no. 04, 2010.
- [11] P. Lichtsteiner, C. Posch and T. Delbruck, "A 128 x 128 120 dB 15 µs Latency Asynchronous Temporal Contrast Vision Sensor," *IEEE Journal of Solid-State Circuits*, vol. 43, no. 2, pp. 566-576, 2008.
- [12] A. Bisulco, F. C. Ojeda, V. Isler and D. D. Lee, "Fast Motion Understanding with Spatiotemporal Neural Networks and Dynamic Vision Sensors," in *2021 IEEE International Conference on Robotics and Automation*, 2020.
- [13] A. Mitrokhin, C. Ye, C. Fermuller, Y. Aloimonos and T. Delbruck, "EV-IMO: Motion Segmentation Dataset and Learning Pipeline for Event Cameras," 2019. [Online]. Available: https://arxiv.org/abs/1903.07520.
- [14] T. Stoffregen, G. Gallego, T. Drummond, L. Kleeman and D. Scaramuzza, "Event-Based Motion Segmentation by Motion Compensation," in *IEEE International Conference on Computer Vision (ICCV)*, Seoul, 2019.
- [15] W. Chamorro, J. Andrade-Cetto and J. Solà, "High Speed Event Camera Tracking," 2020.
- [16] G. Gallego and D. Scaramuzza, "Accurate Angular Velocity Estimation With an Event Camera," *IEEE Robotics and Automation Letters*, 2016.
- [17] H. Kim, S. Leutenegger and A. J. Davison, "Real-Time 3D Reconstruction and 6-DoF Tracking with an Event Camera," vol. 9910, pp. 349-364, 2016.
- [18] G. Gallego, T. Delbrück, G. Orchard, C. Bartolozzi, B. Taba, A. Censi, S. Leutenegger, A. Davison, J. Conradt, K. Daniilidis and D. Scaramuzza, "Event-based Vision: A Survey," 2019.
- [19] J. P. Boettiger, "A Comparative Evaluation of the Detection and Tracking Capability Between Novel Event-Based and Conventional Frame-Based Sensors," 2020.
- [20] Sigma, "70-200mm F2.8 DG OS HSM | Sports Specifications," Sigma Corporation, [Online]. Available: https://www.sigma-global.com/en/lenses/s018_70_200_28/specification.html.
- [21] E. Mueggler, B. Huber and D. Scaramuzza, "Event-based, 6-DOF pose tracking for high-speed maneuvers," in *2014 IEEE/RSJ International Conference on Intelligent Robots and Systems*, 2014.
- [22] H. Rebecq, G. Gallego and D. Scaramuzza, "EMVS: Event-based Multi-View Stereo," in *British Machine Vision Conference (BMVC)*, 2016.

7 ACKNOWLEDGMENT

The authors gratefully acknowledge the help of the Wehrtechnische Dienststelle für Schutz- und Sondertechnik (WTD 52) for providing the test range and their support during the trial. The authors sincerely thank Markus Henriksson and Lars Sjöqvist for their contribution. This work was part of the DeBeLa project, funded by the European Defence Agency.